References

BAILEY, S. W. (1972). *Clays Clay Miner.* **20**, 381–388.
BROWN, B. E. & BAILEY, S. W. (1962). *Am. Mineral.* **47**, 819–850.
BROWN, B. E. & BAILEY, S. W. (1963). *Am. Mineral.* **48**, 42–61.
DORNBERGER-SCHIFF, K. (1964). *Abh. Dtsch. Akad. Wiss. Berlin Kl. Chem. Geol. Biol.* **3**.
ĎUROVIČ, S. (1981). *Fortschr. Mineral.* **59**, 191–226.
ĎUROVIČ, S., DORNBERGER-SCHIFF, K. & WEISS, Z. (1983). *Acta Cryst.* B**39**, 547–552.
JOSWIG, W., FUESS, H., ROTHBAUER, R., TAKÉUCHI, Y. & MASON, S. A. (1980). *Am. Mineral.* **65**, 349–353.
PHILLIPS, T. L., LOVELESS, J. K. & BAILEY, S. W. (1980). *Am. Mineral.* **65**, 112–122.
SHIROZU, H. & BAILEY, S. W. (1965). *Am. Mineral.* **50**, 868–885.
STEINFINK, H. (1958*a*). *Acta Cryst.* **11**, 191–195.
STEINFINK, H. (1958*b*). *Acta Cryst.* **11**, 195–198.
STEINFINK, H. (1962). *Acta Cryst.* **15**, 1310.
WEISS, Z. & ĎUROVIČ, S. (1980). *Acta Cryst.* A**36**, 633–640.

Acta Cryst. (1983). B**39**, 557–561

Electron-Density Distributions in Crystals of $KMnF_3$ and $KNiF_3$

BY NAOTO KIJIMA, KIYOAKI TANAKA AND FUMIYUKI MARUMO

The Research Laboratory of Engineering Materials, Tokyo Institute of Technology, Nagatsuta 4259, *Midori-ku, Yokohama* 227, *Japan*

(*Received* 12 *February* 1983; *accepted* 4 *April* 1983)

Abstract

The electron density distributions in crystals in $KMnF_3$ and $KNiF_3$ were investigated on the bases of the intensity data collected by diffractometry at 293 K. The refinement with aspherical scattering factors for 3*d* orbitals revealed that the Mn^{2+} ion is in the high-spin state $(t_{2g})^3(e_g)^2$ and that the Ni^{2+} ion is in the $(t_{2g})^6(e_g)^2$ state, both to good approximations. Further population refinement showed that the Mn^{2+} ion deviates slightly from the high-spin state and that the Ni^{2+} ion is in the state $(t_{2g})^{5\cdot7}(e_g)^{2\cdot3}$. The residual density map after the population refinement suggests significant anharmonic vibrations of ions in $KMnF_3$ crystals at 293 K. The present study confirms that accurate X-ray diffraction study can detect the difference in 3*d* electron configurations. [Crystal data: $KMnF_3$: *Pm*3*m*, a = 4·1889 (7) Å, $Z = 1$, $D_x = 3{\cdot}412$ g cm^{-3}, μ(Mo $K\alpha$) = 59·35 cm^{-1}; $KNiF_3$: *Pm*3*m*, $a = 4{\cdot}0115$ (7) Å, $Z = 1$, $D_x = 3{\cdot}982$ g cm^{-3}, μ(Mo $K\alpha$) = 88·91 cm^{-1}.]

Introduction

We have performed a series of investigations on electron density distributions in crystals of KMF_3 (*M*: Mn, Fe, Co, Ni and Cu), taking the aspherical distribution of 3*d* electrons into account. In previous articles on $KCuF_3$ (Tanaka, Konishi & Marumo, 1979, 1980) and $KCoF_3$ (Kijima, Tanaka & Marumo, 1981), we have found that residual density maps change drastically according to a slight variation in the assumed configurations of *d* electrons. Distortion of electron distribution by the Jahn–Teller effect in $KCuF_3$ crystals was clearly revealed on deformation density maps. In the case of $KCoF_3$ crystals, the high-spin model deleted most of the peaks around the Co^{2+} ion on the deformation density maps, while the low-spin model gave tremendously large residual peaks. Accordingly it became evident that the spin state of the transition metals could be determined unequivocally by X-ray diffraction.

The present study was undertaken to determine the spin state of the Mn^{2+} ions in $KMnF_3$ crystals and the electron configuration of Ni^{2+} ions in $KNiF_3$ crystals by the X-ray diffraction method.

Experimental

Single crystals of $KMnF_3$ and $KNiF_3$, synthesized by the Bridgemann method and flux method respectively, were used in the present study. They were shaped into spheres by the Bond (1951) method. The lattice constants were determined from 48 2θ values for each crystal. These 2θ values were measured with a four-circle diffractometer using Mo $K\alpha_1$ radiation in the range higher than 88°, where Bragg reflexions of the Mo $K\alpha_1$ and Mo $K\alpha_2$ radiations do not interact with each other. The lattice constants are given in the *Abstract* together with other crystal data. The lattice constants are equal to those observed by Okazaki & Suemune (1961) within the experimental errors.

Intensities of reflexions in an octant of reciprocal space were collected on a Philips automated four-circle diffractometer. As to reflexions with very strong

0108-7681/83/050557-05$01.50

Table 1. *Experimental conditions*

	$KMnF_3$	$KNiF_3$
Diameter of specimen	0·135 mm	0·130 mm
Radiation	Mo $K\alpha$	Mo $K\alpha$
Monochromator	Graphite	Graphite
Collimator	0·5 mm	0·5 mm
$2\theta_{max}$	160°	130°
Scan mode	ω–2θ	ω–2θ
Scan speed	2° min^{-1} in ω	2° min^{-1} in ω
Maximum number of repetitions	10	10
Number of observed reflexions	1019	765
Number of reflexions used	1019	765
Independent reflexions	206	150

intensities, all the equivalent reflexions were measured to assure the subsequent anisotropic extinction corrections. Each reflexion was repeatedly measured up to ten times until the observed intensity exceeded 40000 counts. Scan width was minimized to reduce the statistical counting error and to save time for measurement by changing it according to the equation $A + B \times \tan\theta$, where A and B are suitably chosen constants. In the higher-angle region where Bragg peaks split into the Mo $K\alpha_1$ and Mo $K\alpha_2$ peaks, the wavelength was adjusted to bring the calculated peak position approximately to the midpoint of the two peaks. Other experimental conditions are summarized in Table 1. Absorption correction was performed with the absorption-correction factor A^* taken from *International Tables for X-ray Crystallography* (1967). The mean path length $\bar{T} = (dA^*/d\mu)/A^*$ necessary for the subsequent extinction correction was calculated with the program *DADMYU* written by one of the authors (KT). Here, μ is the linear absorption coefficient, and $dA^*/d\mu$ was calculated by numerical differentiation.

Refinement

$KMnF_3$ and $KNiF_3$ crystals have perovskite-type structures and have no positional parameters to be determined. Refinements were first performed with conventional spherical scattering factors (hereafter abbreviated as SSF) for free ions. Then, by using aspherical scattering factors (hereafter abbreviated as ASF) for 3*d* electrons, electron configurations of the Mn^{2+} and Ni^{2+} ions in the octahedral field were determined in the same way as in the case of $KCoF_3$ (Kijima, Tanaka & Marumo, 1981).

(*a*) *Refinement with SSF*

Atomic scattering factors and dispersion-correction factors for all the constituent ions were taken from *International Tables for X-ray Crystallography* (1974). Before extinction corrections, the discrepancy factors $R_1 = \sum||F_o| - |F_c||/\sum|F_o|$ and $R_2 = [\sum(|F_o| - |F_c|)^2/\sum|F_o|^2]^{1/2}$ were 0·051 and 0·059 for $KMnF_3$, and 0·054 and 0·070 for $KNiF_3$, respectively. Using the method of Becker & Coppens (1974*a*,*b*, 1975), isotropic type I and type II extinction corrections were next performed. The type I extinction correction gave smaller R values for both crystals; the respective R values were 0·014 and 0·015 for $KMnF_3$, and 0·013 and 0·015 for $KNiF_3$. Therefore, the anisotropic extinction corrections of type I were performed subsequently and the R values reduced to 0·012 and 0·012 for $KMnF_3$ and to 0·012 and 0·013 for $KNiF_3$. The maximum corrections applied were those for the 020 reflexions; F_o's on the absolute scale were corrected from 31·91 to 45·52, and from 36·97 to 49·62 for $KMnF_3$ and $KNiF_3$, respectively. Such severe extinction effects were observed also in $KCuF_3$ (Tanaka, Konishi & Marumo, 1979) and $KCoF_3$ crystals (Kijima, Tanaka & Marumo, 1981). In order to avoid interaction of extinction parameters with scale factors and temperature factors, we introduced double scale factors, one for reflexions with $\sin\theta/\lambda \le 0{\cdot}6$ Å^{-1} and the other for reflexions with $\sin\theta/\lambda > 0{\cdot}6$ Å^{-1}. After the extinction correction, the two scale factors became equal within the estimated standard deviations. The atomic and extinction parameters as well as the R_1 factors calculated after averaging the equivalent reflexions are in Tables 2 and 3 for $KMnF_3$ and $KNiF_3$, respectively.

(*b*) *Refinement with ASF*

The scattering factors of the Mn^{2+} and Ni^{2+} ions were assumed as the sums of those of the Ar core and the outer-shell 3*d* electrons. The expressions for the scattering factors of the 3*d* electrons in the octahedral

Table 2. *Anisotropic temperature factors* $[U_{ij}$ (Å^2 × 10^5)], *anisotropic type* I *extinction parameters* $[G_{ij}$ (× 10^4)], *population* (p) *and R values for* $KMnF_3$

Mn^{2+}, K^+ and F^- ions occupy the sites (0,0,0), ($\frac{1}{2},\frac{1}{2},\frac{1}{2}$) and ($\frac{1}{2}$,0,0), respectively. The form of the anisotropic temperature factor is defined as $\exp[-2\pi^2a^{*2}(h^2 + k^2 + l^2)\,U_{11}]$ for Mn^{2+} and K^+, and $\exp\{-2\pi^2a^{*2}[h^2U_{11} + (k^2 + l^2)\,U_{22}]\}$ for F^-.

Type of refinement		(*a*) $(t_{2g})^3(e_g)^2$ (spherical)	(*b*-1) $(t_{2g})^5$	(*b*-2) $(t_{2g})^{2\cdot89}(e_g)^{2\cdot11}$
Mn	p			0·11 (7)
	U_{11}	754 (2)	751 (3)	750 (2)
K	U_{11}	1989 (5)	1998 (7)	1992 (5)
F	U_{11}	777 (12)	795 (17)	779 (12)
	U_{22}	3518 (21)	3472 (29)	3523 (21)
G_{11}		889 (15)	916 (22)	902 (15)
G_{22}		2336 (75)	2761 (115)	2372 (76)
G_{33}		937 (16)	958 (23)	951 (16)
G_{12}		161 (33)	216 (50)	164 (33)
G_{13}		−109 (14)	−137 (21)	−110 (14)
G_{23}		19 (29)	40 (44)	21 (29)
R_1		0·0098	0·0203	0·0097

Table 3. *Anisotropic temperature factors* [U_{ij} (Å^2 × 10^5)], *anisotropic type* I *extinction parameters* [G_{ij} (× 10^4)], *population* (*p*) *and R values for* $KNiF_3$

Ni^{2+}, K^+ and F^- ions occupy the sites (0,0,0), ($\frac{1}{2},\frac{1}{2},\frac{1}{2}$) and ($\frac{1}{2}$,0,0), respectively. The form of the anisotropic temperature factors is defined as $\exp[-2\pi^2a^{*2}(h^2 + k^2 + l^2)U_{11}]$ for Ni^{2+} and K^+, and $\exp\{-2\pi^2a^{*2}[h^2U_{11} + (k^2 + l^2)U_{22}]\}$ for F^-.

Type of refinement		(*a*) $(t_{2g})^{4\cdot8}(e_g)^{3\cdot2}$ (spherical)	(*b*-1) $(t_{2g})^6(e_g)^2$	(*b*-2) $(t_{2g})^{5\cdot70}(e_g)^{2\cdot30}$
Ni	*p*			0·30 (8)
	U_{11}	491 (2)	485 (2)	485 (2)
K	U_{11}	1197 (5)	1200 (5)	1200 (4)
F	U_{11}	548 (13)	558 (13)	556 (12)
	U_{22}	1492 (14)	1478 (13)	1482 (13)
G_{11}		298 (24)	301 (23)	302 (22)
G_{22}		324 (24)	343 (23)	340 (22)
G_{33}		294 (8)	301 (8)	301 (8)
G_{12}		35 (7)	39 (6)	39 (6)
G_{13}		61 (11)	68 (10)	67 (10)
G_{23}		95 (11)	97 (10)	97 (10)
R_1		0·0116	0·0080	0·0079

field were given by Tanaka, Konishi & Marumo (1979, 1980). The scattering factors of the Ar core and the orbital scattering factors of the 3*d* electrons, $\langle j_0\rangle_{3d}$, $\langle j_2\rangle_{3d}$ and $\langle j_4\rangle_{3d}$ were taken from *International Tables for X-ray Crystallography* (1974). The refinement was performed with the program *LINKT* written by one of the authors (KT).

Refinements for $KMnF_3$ with ASF were performed by assuming (*b*-1) low-spin $(t_{2g})^5$ and (*b*-2) intermediate $(t_{2g})^{3-p}(e_g)^{2+p}$ electron configurations. The parameter *p* was determined in the least-squares calculation to be 0·11 (7). Other parameters are in Table 2.

Refinements for $KNiF_3$ crystals were performed with two electron-configuration models, (*b*-1) $(t_{2g})^6(e_g)^2$ and (*b*-2) $(t_{2g})^{6-p}(e_g)^{2+p}$. The value of *p* was determined to be 0·30 (8). Parameters obtained are in Table 3.*

Results and discussion

A spherical-atom model of metal atoms corresponds to equal occupation of 3*d* electrons in the five 3*d* orbitals. In this case, the coefficients of $\langle j_2\rangle_{3d}$ and $\langle j_4\rangle_{3d}$ are summed to zero and only the term of $\langle j_o\rangle_{3d}$ without angular components remains. Thus the high-spin $(t_{2g})^3(e_g)^2$ model of the Mn^{2+} ion is expected to show spherical electron distribution. The spherical-atom model of the Ni^{2+} ion corresponds to the $(t_{2g})^{4\cdot8}(e_g)^{3\cdot2}$ state. In Table 4, electron populations of t_{2g} and e_g orbitals in d^4 to d^7 metals in octahedral fields are summarized for high- and low-spin states, and for the spherical model. It is evident that populations of t_{2g} are always larger in both high- and low-spin states than those in the spherical model except for the d^5 case, and *vice versa* for e_g orbitals. Accordingly it is impossible to assign the spin state unequivocally without making use of the ASF refinement.

Figs. 1(*a*) and 1(*b*) show the deformation density around the Mn^{2+} ion after the refinement with SSF. Positive peaks with heights 0·38 e Å^{-3} lie at 0·37 Å from the Mn nucleus along ⟨100⟩. Negative peaks with depths −0·36 e Å^{-3} lie at 0·36 Å away from the Mn nucleus along ⟨111⟩. Fig. 2 shows the residual density

Table 4. *Electron populations in* t_{2g} *and* e_g *orbitals of high- and low-spin transition metals and those of the corresponding spherical-atom models*

		d^4	d^5	d^6	d^7
High spin	t_{2g}	3	3	4	5
	e_g	1	2	2	2
Low spin	t_{2g}	4	5	6	6
	e_g	0	0	0	1
Spherical	t_{2g}	2·4	3	3·6	4·2
	e_g	1·6	2	2·4	2·8

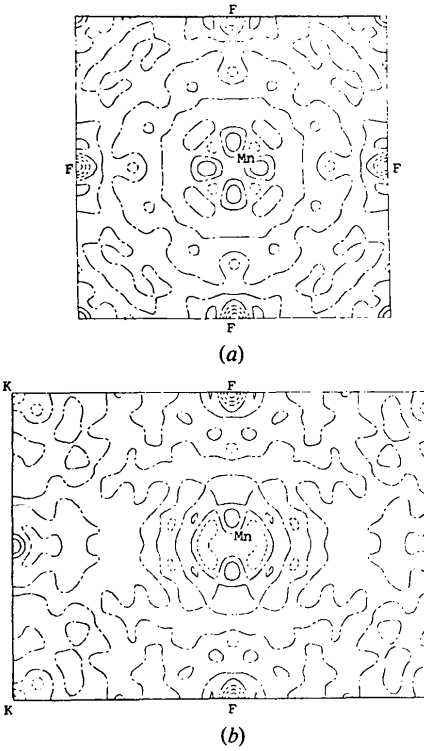

Fig. 1. Sections of the difference Fourier map around Mn^{2+} after the SSF refinement on the planes (*a*) *z* = 0 and (*b*) *x* = *y*. Contours are at intervals of 0·2 e Å^{-3}. Negative and zero contours are in broken and dashed–dotted lines, respectively.

* A list of structure factors has been deposited with the British Library Lending Division as Supplementary Publication No. SUP 38493 (16 pp.). Copies may be obtained through The Executive Secretary, International Union of Crystallography, 5 Abbey Square, Chester CH1 2HU, England.

obtained with the low-spin model $(t_{2g})^5$. Large positive peaks with heights 2·47 e Å^{-3} lie at 0·42 Å from the Mn nucleus along ⟨100⟩, and large negative peaks with depths −1·61 e Å^{-3} lie at 0·41 Å from the Mn nucleus along ⟨111⟩. It is evident from these values that the Mn^{2+} ion in $KMnF_3$ is not in the low-spin state. However, the positive peaks on the Mn—F bonds in Fig. 1 indicate that the population of the e_g orbitals is expected to be a little larger than the value for the high-spin state. Therefore, the populations of t_{2g} and e_g orbitals were refined assuming the $(t_{2g})^{3-p}(e_g)^{2+p}$ electron configuration. The refinement gave the value 0·11 (7) for p, and reduced heights of the positive peaks along ⟨100⟩ on the difference Fourier map to 0·29 e Å^{-3} and the depths of the negative peaks along ⟨111⟩ to −0·28 e Å^{-3} with respect to the values in Fig. 1. However, unsatisfactory improvements of the residual density map and R factors as well as the p value comparable to its e.s.d. in magnitude indicate that other sources should be sought to explain these peaks. Since the symmetry of the Mn^{2+} site is $m3m$, two independent fourth-order anharmonic parameters are permitted after Willis's (1969) formalism of anharmonic vibration. They correspond to the vibration along Mn—F bonds and along the directions bisecting the Mn—F bonds in {001}. Thus, positive peaks on the deformation density map (Fig. 1) may be due to the negative anharmonic potential along the Mn—F bonds. The analysis of anharmonic vibration in $KMnF_3$ crystals will be presented elsewhere (Tanaka & Marumo, 1983).

The deformation density around the Ni^{2+} ions in $KNiF_3$ crystals after the refinement with SSF is shown in Figs. 3(*a*) and 3(*b*). Negative peaks with depths −1·25 e Å^{-3} lie at 0·43 Å from the Ni nucleus along ⟨100⟩ in Fig. 3(*a*). There are positive peaks with heights 0·93 e Å^{-3} at 0·45 Å from the Ni nucleus along ⟨111⟩ in Fig. 3(*b*). Fig. 3(*b*) shows similar features as found for γ-Ni_2SiO_4 in which the Ni^{2+} ion is in a trigonally distorted octahedral field (Marumo, Isobe, Saito, Yagi & Akimoto, 1974).

Fig. 4 shows the residual density after the refinement with ASF assuming $(t_{2g})^6(e_g)^2$. The negative peaks on the Ni—F bonds along ⟨100⟩ in Fig. 3(*a*) have disappeared and, instead, positive peaks with heights 0·35 e Å^{-3} appear at distances of 0·38 Å from the Ni nucleus. The positive peaks along ⟨111⟩ and at the Ni nucleus in Figs. 3(*a*) and 3(*b*) have also disappeared in Fig. 4. These changes as well as the significant reduction of the R_1 factor from 0·012 to 0·008 indicate definitely that the peaks in Figs. 3(*a*) and 3(*b*) around the Ni^{2+} ion are all due to aspherical

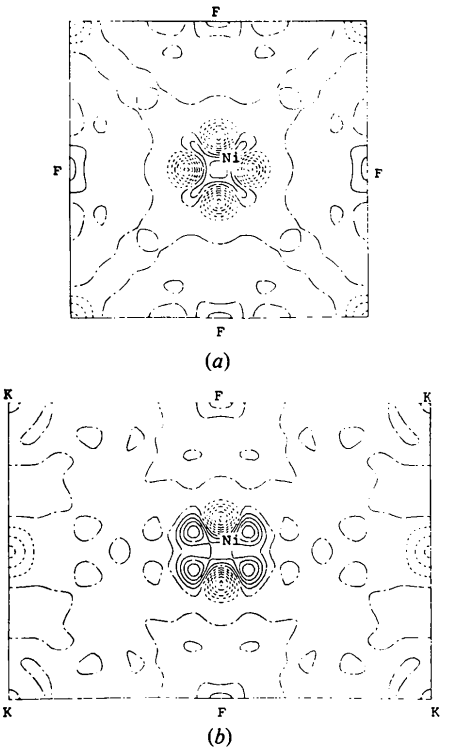

Fig. 3. Sections of the difference Fourier map around Ni^{2+} after the SSF refinement on the planes (*a*) $z = 0$ and (*b*) $x = y$ and with the same intervals as in Fig. 1.

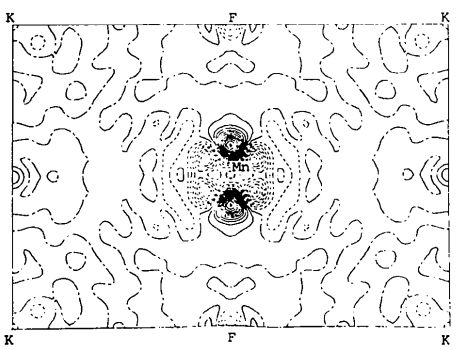

Fig. 2. A section of the difference Fourier map around Mn^{2+} after the ASF refinement assuming the low-spin $(t_{2g})^5$ state on the plane $x = y$ and with the same intervals as in Fig. 1.

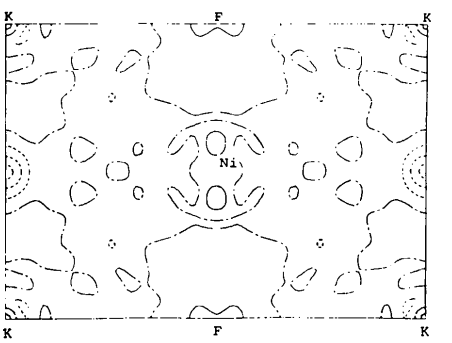

Fig. 4. A section of the difference Fourier map around Ni^{2+} after the ASF refinement on the plane $x = y$ and with the same intervals as in Fig. 1.

3*d* electron distributions and that $(t_{2g})^6(e_g)^2$ is a good approximation for the 3*d* electron configuration in the Ni^{2+} ion. However, the remaining peaks in Fig. 4 indicate also that the population of e_g orbitals, which extend toward ligands, may be a little larger than 2. By the population refinement with the model $(t_{2g})^{6-p}(e_g)^{2+p}$, we obtained 0·30 (8) for *p*. The deformation density map after this refinement shows that the positive peaks in Fig. 4 have disappeared and there remains no significant peak around the Ni^{2+} ion.

Conclusion

With the X-ray diffraction technique, the Mn^{2+} ion in $KMnF_3$ crystals was confirmed to be in the high-spin state in the same way as applied to the Co^{2+} ion in $KCoF_3$ crystals (Kijima, Tanaka & Marumo, 1981). The large difference between the residual densities in Figs. 1 and 2, and between those in Figs. 3 and 4 assure that a careful X-ray study is accurate enough to detect the difference of the electron configurations in transition metals. The X-ray diffraction method may be applied also to mixed-valence complexes and to many other compounds where the determination of the electron configuration of transition metals is important.

The authors wish to express their sincere gratitude to Professor M. Kato of Tokyo Institute of Technology for supplying facilities for data collection. Our thanks are also due to Professors A. Ito and H. Ikeda of Ochanomizu University, and to Professor A. Okazaki of Kyushu University for kindly supplying crystal specimens. We are indebted to Drs M. Sano and E. Miyoshi and Professor H. Kashiwagi for supplying the program *JGRAPH*. One of the authors (NK) wrote the program *FRPLOT* on the basis of *JGRAPH*. All the difference Fourier maps were depicted by *FRPLOT*. Part of the cost was met by a Scientific Research Grant from The Ministry of Education, Science and Culture, to which the authors' thanks are due.

References

BECKER, P. J. & COPPENS, P. (1974*a*). *Acta Cryst.* A**30**, 129–147.
BECKER, P. J. & COPPENS, P. (1974*b*). *Acta Cryst.* A**30**, 148–153.
BECKER, P. J. & COPPENS, P. (1975). *Acta Cryst.* A**31**, 417–425.
BOND, W. L. (1951). *Rev. Sci. Instrum.* **22**, 344.
International Tables for X-ray Crystallography (1967). Vol. II, 2nd ed. Birmingham: Kynoch Press.
International Tables for X-ray Crystallography (1974). Vol. IV. Birmingham: Kynoch Press.
KIJIMA, N., TANAKA, K. & MARUMO, F. (1981). *Acta Cryst.* B**37**, 545–548.
MARUMO, F., ISOBE, M., SAITO, Y., YAGI, T. & AKIMOTO, S. (1974). *Acta Cryst.* B**30**, 1904–1906.
OKAZAKI, A. & SUEMUNE, Y. (1961). *J. Phys. Soc. Jpn*, **16**, 671–675.
TANAKA, K., KONISHI, M. & MARUMO, F. (1979). *Acta Cryst.* B**35**, 1303–1308.
TANAKA, K., KONISHI, M. & MARUMO, F. (1980). *Acta Cryst.* B**36**, 1264.
TANAKA, K. & MARUMO, F. (1983). To be published.
WILLIS, B. T. M. (1969). *Acta Cryst.* A**25**, 277–300.

Acta Cryst. (1983). B**39**, 561–564

Electron Density Distribution in Crystals of Iron(II) Potassium Trifluoride

BY NOBORU MIYATA, KIYOAKI TANAKA AND FUMIYUKI MARUMO

The Research Laboratory of Engineering Materials, Tokyo Institute of Technology, Nagatsuta 4259, *Midori-ku, Yokohama* 227, *Japan*

(*Received* 24 *February* 1983; *accepted* 25 *April* 1983)

Abstract

The electron density distribution in a crystal of $KFeF_3$ was investigated on the basis of X-ray intensity data collected by diffractometry at 298 K. The deformation densities around the Fe^{2+} ion in an octahedral field were analysed by utilizing aspherical scattering factors. The refinement assuming the high-spin state for the Fe^{2+} ion decreased the *R* value to 0·0072 from the 0·0075 obtained with spherical scattering factors, while that assuming the low-spin state increased the value to 0·0142. Further, the refinement of electron populations for t_{2g} and e_g orbitals gave the electronic state as $(t_{2g})^{3\cdot93}(e_g)^{2\cdot07}$. The difference Fourier maps after these refinements also showed that the high-spin model is a good approximation to the electronic state of the Fe^{2+} ion in the cubic $KFeF_3$ crystal at room temperature. [Crystal data: M_r = 151·95, cubic, $Pm3m$, a = 4·1198 (1) Å, V = 69·924 Å^3, Z = 1, D_x = 3·60 g cm^{-3}, μ(Mo $K\alpha_1$) = 90·89 cm^{-1}.]

0108-7681/83/050561-04$01.50